The mechanics of a ping-pong ball gun

Article *in* Experimental Techniques · May 2007

DOI: 10.1111/j.1747-1567.2007.00214.x

4 authors, including:

Mark French
Purdue University
95 PUBLICATIONS **191** CITATIONS
SEE PROFILE

Vijay Gorrepati
The University of Chicago Medical Center
1 PUBLICATION **1** CITATION
SEE PROFILE

Mark James Jackson
Kansas State University
327 PUBLICATIONS **1,291** CITATIONS
SEE PROFILE

by R.M. French, V. Gorrepati, E. Alcorta, and M. Jackson

THE MECHANICS OF A PING-PONG BALL GUN

A vacuum-powered ping-pong ball gun has been used as a very compelling demonstration device in physics and mechanics classes.[1,2] It shoots ping-pong balls with a muzzle velocity that can exceed 700 feet/s—enough to shoot through several (empty) aluminum soda cans (see Fig. 1). One of us (MF) has successfully used the ping-pong gun to teach principles of dynamics in undergraduate classes. However, using the device in class inspired some specific questions about how it works.

The gun is simply a long tube with sealed ends, from which most of the air has been removed. As shown in Fig. 2, the gun is fired by puncturing the seal on one end. Air at atmospheric pressure rushes in through the now open end of the tube, driving the ping-pong ball ahead of it. A moving ping-pong ball normally slows quickly because of aerodynamic drag, but there is no air ahead of the ball. Thus, it accelerates quickly down the tube. The inner diameter of the tube is slightly larger than the outer diameter of the ball, so a small amount of air slips past the ball as it accelerates toward the muzzle. When it reaches the muzzle, this small air charge is compressed between the oncoming ball and the seal, and the resulting pressure increase ruptures the seal. The ball then exits through the unobstructed muzzle.

Figure 3 shows high-speed video images of a typical firing. The three frames are immediately before impact of the ball with a soda can, impact, and immediately after impact. The frames were taken 1/1000 s apart with an exposure time of 1/4000 s. The second frame shows the ball emerging from the can and the third frame shows the tape in motion toward the can. We often mark the breech and muzzle seals with different colored permanent markers so that the tape fragments can be identified after a shot.

The gun is made from a 10-foot piece of 1.5 inches schedule 40 polyvinyl chloride (PVC) tubing. The inner diameter of the tube is slightly larger than the 40-mm outside diameter of a ping-pong ball. The tube is fitted with Plexiglas end plates and sealed using 3-inch-wide packing tape. The end plates both support the tube and provide a good surface for the tape as shown in Fig. 4.

A first-order analysis by Ayars and Buchholtz[3] suggests that maximum muzzle velocity is less than the speed of sound and that the gun can approach this value asymptotically with increasing barrel length. They define initial acceleration, a_0, of the ball as follows:

$$a_0 = \frac{F}{m} = \frac{P_0 A}{m} \tag{1}$$

where P_0 is atmospheric pressure, A is the cross-sectional area of the ball, and m is the mass of the ball. They define a characteristic length, λ, as follows:

$$\lambda = \frac{m}{\rho A} \tag{2}$$

where ρ is air density. The resulting expression for velocity as a function of distance down the tube is then

$$v(x) = v_{\max}\left[\frac{x}{x+\lambda}\sqrt{1+\frac{2\lambda}{x}}\right] \tag{3}$$

where

$$v_{\max} = \sqrt{a_0 \lambda} = \sqrt{\frac{P_0}{\rho}} \tag{4}$$

The ball is 40 mm in diameter, so $A = 0.0012566$ m^2. Nominally, $P_0 = 101{,}300$ Pa and $\rho = 1.225$ kg/m^3, so $v_{\max} = 287.6$ m/s. Finally, a typical ball weighs approximately 2.3 g. The resulting predicted velocity profile along the barrel is shown in Fig. 5.

Note that the predicted velocity asymptotically approaches a maximum of approximately 287 m/s. This is due to the increasing mass of air behind the ball that must be accelerated to the speed of the ball as it moves down the barrel. Ayarsa and Buchholtz also give an expression for the velocity of the ball as a function of time.

$$v(t) = \frac{a_0 t}{\sqrt{1+\frac{a_0 t^2}{\lambda}}} = \frac{v_{\max}}{\sqrt{1+\frac{\lambda}{a_0 t^2}}} \tag{5}$$

Figure 6 shows that the maximum velocity is reached in about 20 msec. Finally, the predicted position in the barrel as a function of time is as follows:

$$x(t) = \lambda\left[\sqrt{1+\frac{a_0 t^2}{\lambda}} - 1\right] \tag{6}$$

Figure 7 shows the position of the ball as a function of time. In this paper, we describe our work to more accurately model the flow inside the barrel and to verify the results experimentally.

ANALYSIS

Describing the flow inside the barrel during firing is challenging because it is dominated by features that are often omitted for the sake of mathematical simplicity. The flow is transient and compressible. The geometric boundary conditions change rapidly with time. The annular gap between the ball and the

R. M. French is an Assistant Professor, V. Gorrepati is a graduate student, E. Alcorta is a graduate student, and M. Jackson is an Associate Professor with the Department of Mechanical Engineering Technology at Purdue University, West Lafayette, IN.

doi: 10.1111/j.1747-1567.2007.00214.x

Fig. 1: Aluminum soda cans used as targets

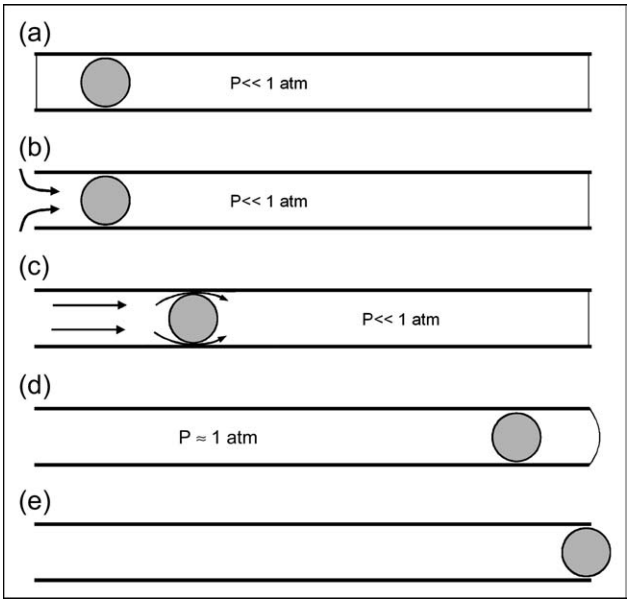

Fig. 2: Mechanics of firing (a) tube is evacuated with end seals in place, (b) seal is punctured and air rushes into vacuum, (c) pressure differential accelerates ball and some air leaks past, (d) air ahead of the ball is compressed and breaks muzzle seal, and (e) ball exits through open muzzle

barrel is small enough that viscosity cannot be ignored. Clearly, a precise description of the flow requires a computational fluid dynamic (CFD) analysis.

We used FLUENT[4] to analyze the flow inside the gun. Modeling the flow around a fixed ball is relatively simple, but the moving boundary condition created by the ball cannot be ignored. For our analysis, the ball moves under the influence of the calculated aerodynamic forces. FLUENT supports this capability, though it is not a standard feature of the software. Rather, a user-defined function had to be written to account for motion of the ball.

In addition, the analytical mesh has to move in accordance with the calculated ball motion. Dynamic mesh motion is a standard part of the software, and the volume immediately around the ball was defined to move with it. Most of the barrel was modeled with a fixed mesh; only the mesh for the ball and zone immediately around it moved. At the boundary between the dynamic and the fixed portions of the mesh, grid points were either generated or absorbed as necessary. Figure 8 shows the mesh immediately surrounding the ball. We assumed a ball diameter of 40 mm and an inner tube diameter of 44 mm.

Because the geometry is axisymmetric, we were able to compute the solution with many fewer grid points than would be required for a complete three-dimensional model. Our axisymmetric model has approximately 2000 grid points. We used a very small time step, $\Delta t = 0.0001$ s, to capture the details of the highly transient behavior of the flow around the ball. We allowed 100 iterations per time step and monitored computational residuals to ensure the calculation converged at each time step.

Figure 9 shows the calculated velocity contours around the ball at $t = 0.001$, $t = 0.002$, $t = 0.003$, and $t = 0.009$ s. The scale on the left side of the figure is the velocity in meter per second. The top three images show the pressure pulse from the burst diaphragm reaching the ball. They also

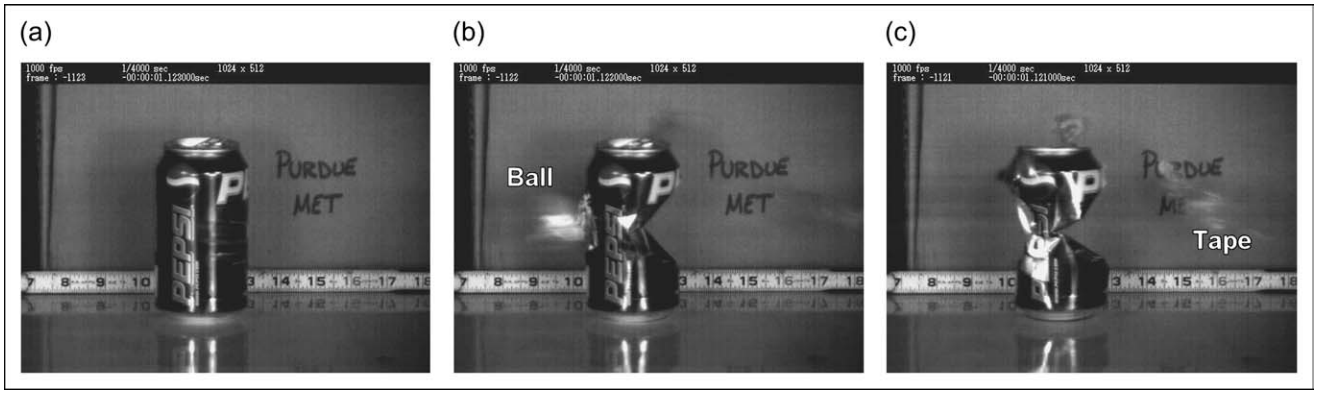

Fig. 3: Impact of ball at (a) t = 0.000 s, (b) t = 0.001 s, and (c) t = 0.002 s

Fig. 4: Muzzle and target cans

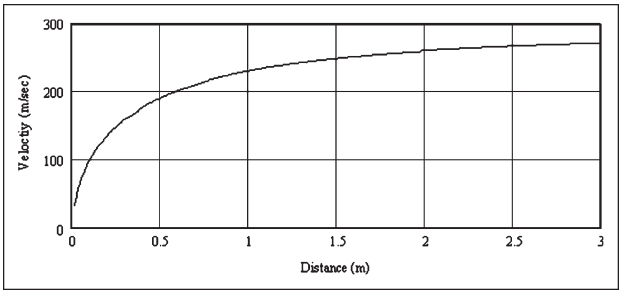

Fig. 5: Predicted velocity along the barrel using analytical model

show the boundary layer developing. The fourth image shows a low-velocity area immediately in front of the ball and high-speed flow in the annular region between the ball and the tube walls. This is analogous to the normal shock at the throat of a conventional axisymmetric convergent–divergent nozzle.[5] The flow is this area is well in excess of the speed of sound, which is approximately 334 m/s at sea level.

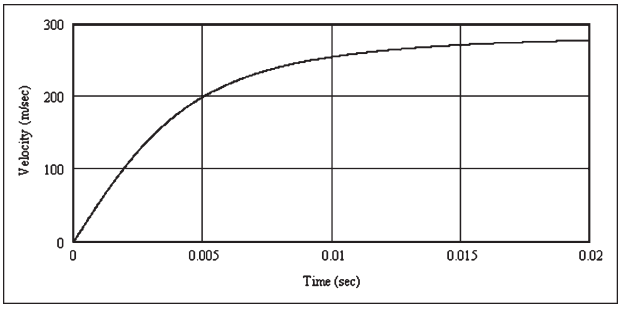

Fig. 6: Predicted velocity versus time using analytical model

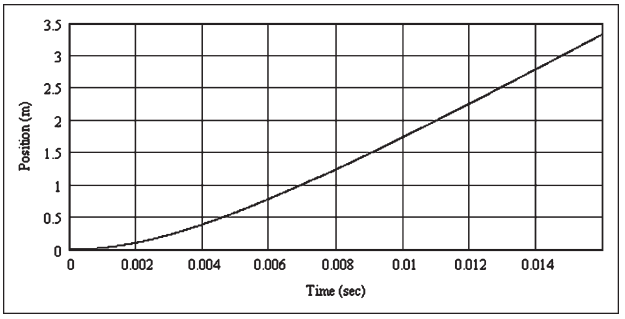

Fig. 7: Predicted position versus time using analytical model

The total pressure contours around the ball at the same points in time are shown in Fig. 10. The scale is in the fraction of atmospheric pressure, so that lightest isopressure line corresponds to one atmosphere. The pressure near the ball is essentially zero until the fourth frame in the series. As one would expect, the topology of the isopressure lines largely matches those of the velocity lines. At the flow develops, a high-pressure zone builds around the front of the ball.

Figure 11 shows the calculated velocity of the ball as a function of its position in the barrel.

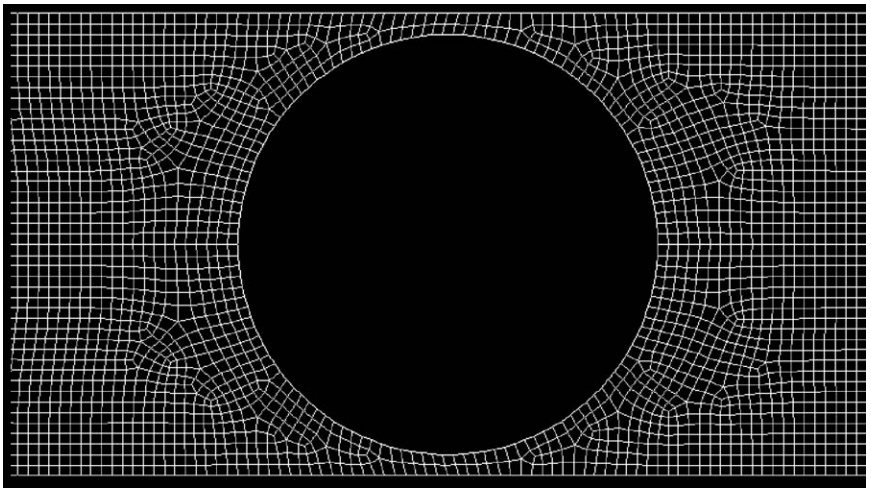

Fig. 8: Mesh immediately surrounding the ball

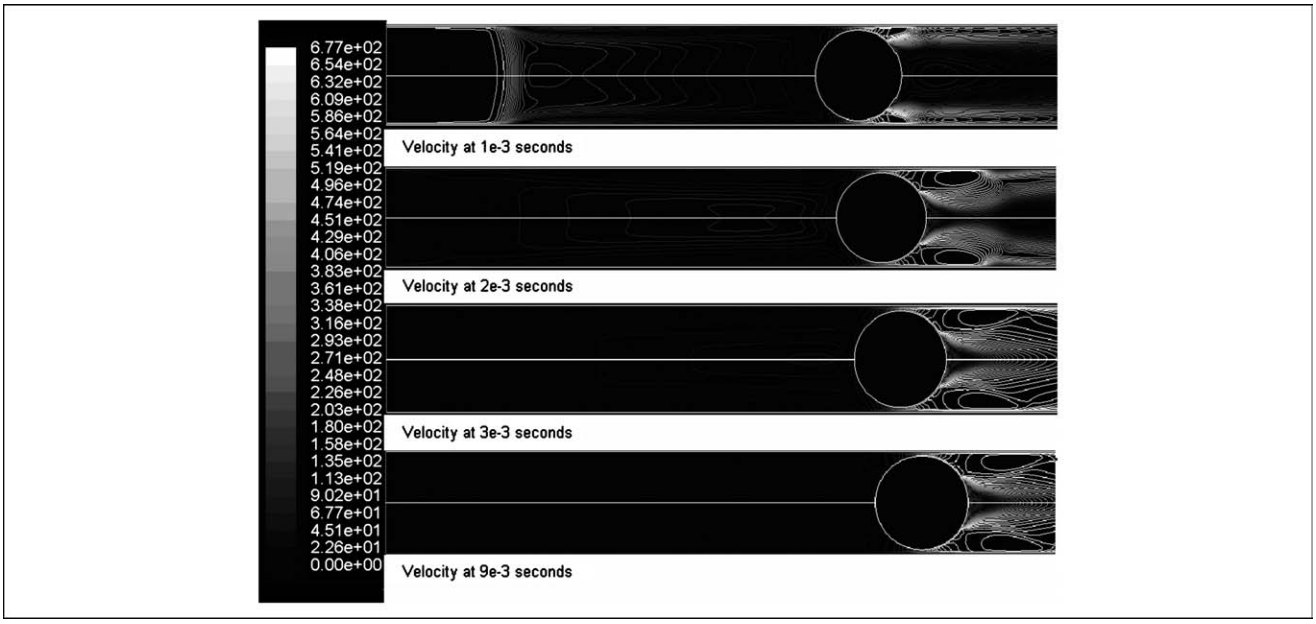

Fig. 9: Velocity contours around the ball

EXPERIMENTAL VERIFICATION

The analytical and numerical results are based on the gun as shown in Fig. 12. It is made from a 10-foot (3.05 m) section of 1.5 inches, schedule 40 PVC pipe of the type often used for plumbing in houses. The gun is supported by flat end plates and two other blocks along the barrel—a necessity because the PVC tube is flexible and cannot support its own weight without sagging.

The barrel is fitted with a Piezotronics PCB pressure sensor (Depew, NY) and several optical windows along its length. We mounted laser diodes and high-speed photodetectors on three windows along the barrel so the ball passage could be detected. The barrel was evacuated with a two-stage vacuum pump that typically generated a 98% vacuum (as measured by an SMC Corporation of America digital gage [Indianapolis, IN]). This corresponds to an absolute internal pressure of

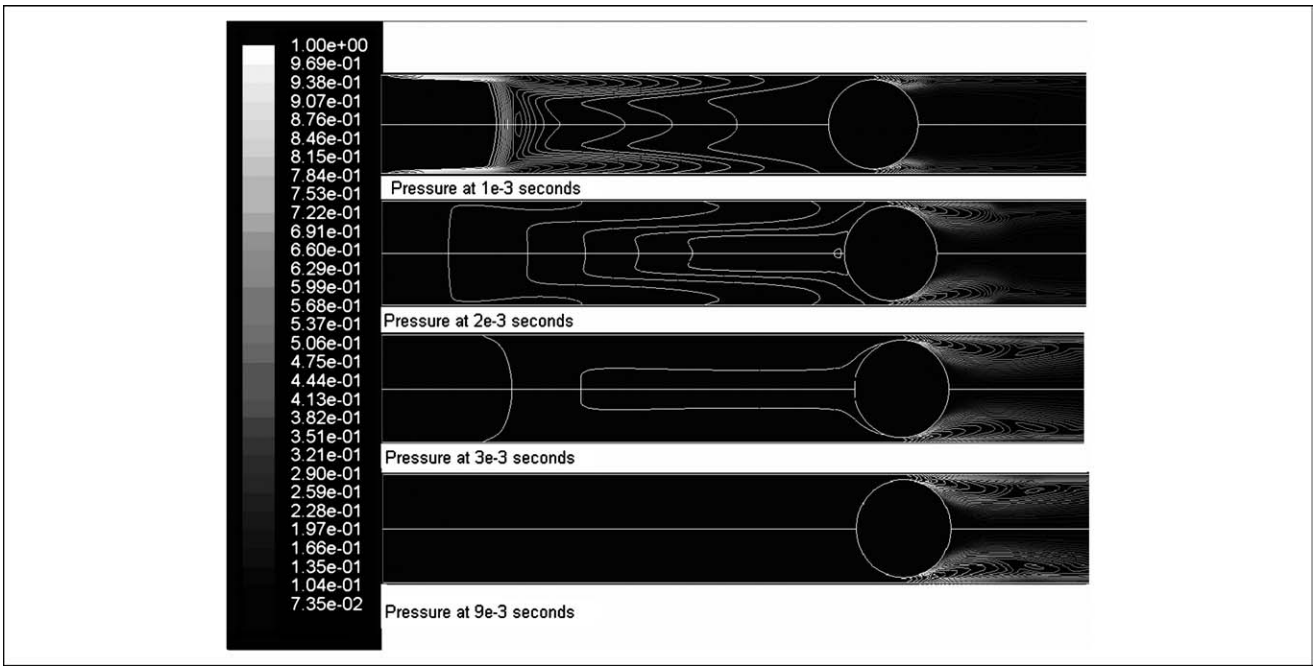

Fig. 10: Total pressure around the ball at $T = 0.0105$ s

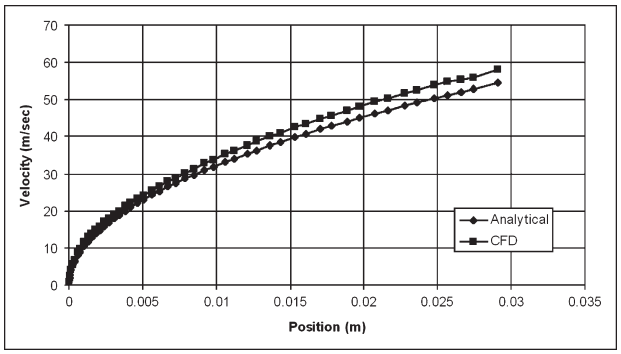

Fig. 11: Velocity versus distance from computational fluid dynamic calculation

about 0.3 psi (2.07 kPa). It is important to note that the gun will not fire if the internal pressure is too high. A typical single-stage vacuum pump, sometimes called a roughing pump, will not reduce the internal pressure enough for the gun to fire. Figure 13 shows a diagram of the test system.

Our tests on a 10-foot (3.05 m) barrel yielded a muzzle velocity of up to 650 feet/s (198 m/s). The variation in muzzle is large (on the order of ±50 feet/s) and appears to be due to the method of puncturing the breech seal. For convenience, we puncture the seal using a sharp knife. The resulting orifice size varies from a complete circle roughly the diameter of the tube to a half circle as shown in Fig. 14. One of our future developments will be a device to more repeatably puncture the breech seal.

Figure 15 shows a typical set of signals from the photodetectors. It is clear that the time between the photodetectors decreases as the ball moves down the barrel and that the time the ball obscured each detector also decreased. Because the ball diameter is 40 mm and we assume it does not significantly deform during acceleration, the three detectors yield five data points: $t_{1\text{–}2}$, $t_{2\text{–}3}$, Δt_1, Δt_2 and Δt_3. This data provides two known positions as a function of time and three velocities at known positions and times. Note that there are only two known positions as a function of time since the times are referenced to the time at which the ball crosses the first detector. The time between the firing and the ball crossing the first detector is unknown. Velocity at the three detector points is determined by dividing the diameter of the ball by the time each detector was obscured.

Figure 16 shows the analytical prediction for velocity as a function of position along with experimental values. The variation in the measured velocities is largely due to the sample rate of the data acquisition system. We sampled our data at 51200 Hz—the maximum rate for our system. However, a higher rate would have reduced the uncertainty in velocity. At this sample rate, $\Delta t = 1.953 \times 10^{-5}$ s. This results in an uncertainty in velocity that is a function of the velocity. If the time required for the ball to pass the photodetector is $n\Delta t$ (where n is an integer), then the velocity of the ball is as follows:

$$V = \frac{d}{n\Delta t} \tag{7}$$

where d is the diameter of the ball. If the uncertainty in time is $\pm\Delta t/2$, then there are two expressions for the resulting uncertainty in velocity.

$$\begin{aligned} \Delta V^- &= \frac{d}{(n+\frac{1}{2})\Delta t} - \frac{d}{n\Delta t} = \frac{-d}{2n(n+\frac{1}{2})\Delta t} \approx \frac{-d}{2n^2\Delta t} \qquad \text{for } n >> 1 \\ \Delta V^+ &= \frac{d}{(n-\frac{1}{2})\Delta t} - \frac{d}{n\Delta t} = \frac{d}{2n(n-\frac{1}{2})\Delta t} \approx \frac{d}{2n^2\Delta t} \qquad \text{for } n >> 1 \end{aligned} \tag{8}$$

We noticed an interesting feature in the pressure data as shown in Fig. 17. After the ball exited the barrel, there was a low-amplitude oscillation of the air pressure in the barrel. The data presented here have been filtered to remove the low-frequency components that dominate the signal. The period is approximately $T = 0.018$ s. This would appear to be the resonant oscillation of the air column in the barrel. The expression for the resonant frequencies of an open tube in air is as follows:

$$f = \frac{nc}{2L} \tag{9}$$

where n is an integer greater than zero, c is the speed of sound in air, and L is the length of the barrel. Assuming a standard atmosphere, $c = 1118$ feet/s (340.9 m/s), the predicted fundamental period for a 10-foot tube is 55.9 Hz. The resulting

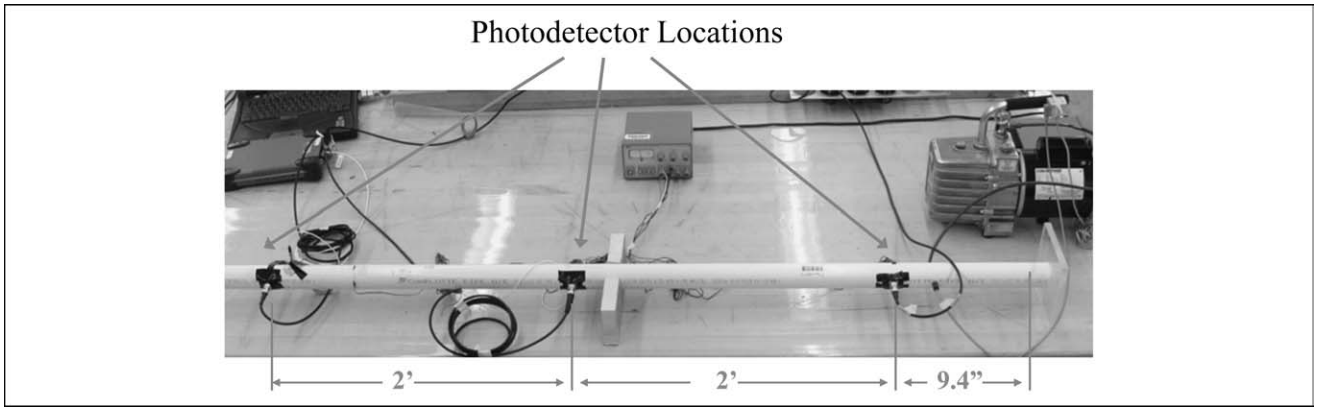

Fig. 12: Barrel with optical sensors

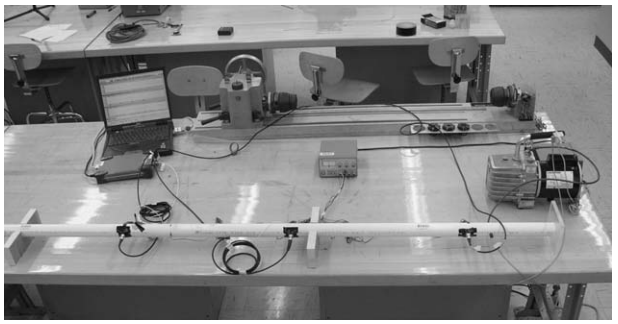

Fig. 13: Diagram of test setup

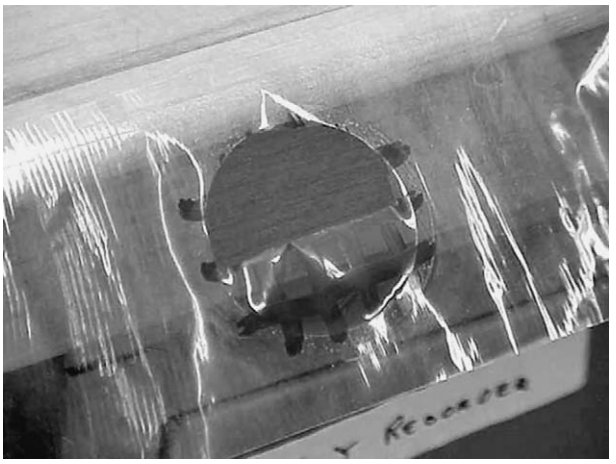

Fig. 14: Breech seal after firing

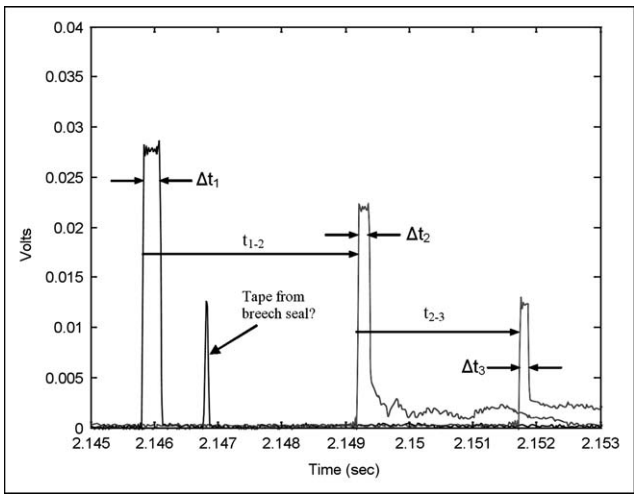

Fig. 15: Typical data from optical sensors

period is 0.0179 s. It seems clear that this trailing oscillation is simply the decaying response of the air column in the tube. This feature might provide a secondary means of verifying a CFD analysis that modeled the ball moving all the way down the tube and exiting at the muzzle.

A final observation based on high-speed video from many firings is that the gun recoils. Between the time at which the

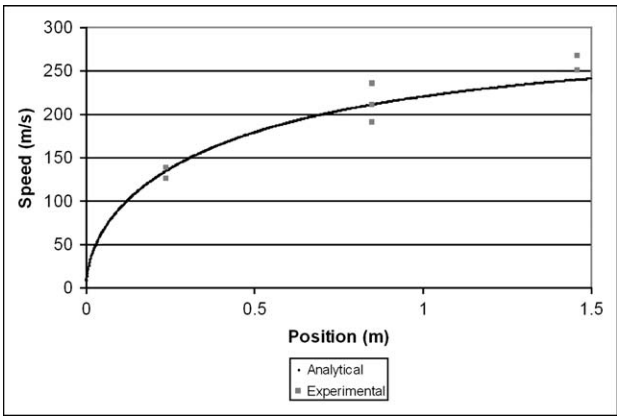

Fig. 16: Experimental results versus first-order analysis

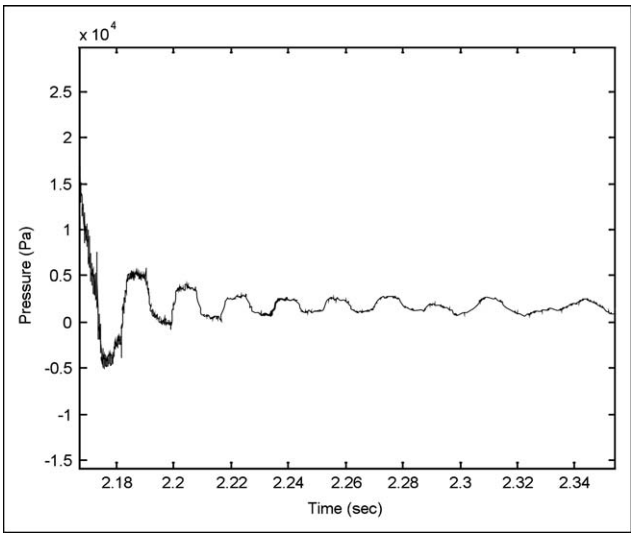

Fig. 17: High pass–filtered data from pressure sensor

breech seal is punctured and the time the ball exits the muzzle, the barrel clearly moves backwards—the reverse of the direction the ball is traveling. We speculate that recoil is due to the pressure differential between the muzzle seal, which is still in place at this phase of firing, and the open breech, which is vented to the atmosphere. So far, we have only fired the gun sitting on a smooth tabletop. It would be interesting to suspend the gun using a parallelogram linkage or perhaps light string to allow it to recoil freely without friction from the tabletop.

CONCLUSIONS

The vacuum-powered ping-pong ball gun provides a compelling demonstration of dynamics in the classroom. However, the underlying physics are subtle and a rich source of fluid-structure interaction phenomena. We have instrumented a large ping-pong gun, collecting time-dependent pressure data, position and velocity data from the ball, and high-speed video of impact with a number of different targets.

We compare the experimental results with both analytical predictions from the literature and our own CFD model of the firing event. Computation and experiment are well correlated.

In addition, we have identified phenomena that hint at the complex physics underlying the gun's operation. There is clearly transonic and supersonic flow within the barrel, and there is a trailing pressure oscillation that appears to be the fundamental resonance of the air column in the open-ended tube and the gun clearly recoils.

We plan to improve the gun using a better means of puncturing the breech seal, and also hope to increase its muzzle velocity by changing the barrel geometry.

ACKNOWLEDGMENTS

We wish to acknowledge the support of the Partners for Advanced Collaborative Engineering Education program for providing access to FLUENT. Professor John Cockman at Appalachian State University provided useful advice in getting our initial gun to work correctly. SMC Corp. provided a digital pressure gage.

References

1. Peterson, R.W., Pulford, B.N., and Stein, K.R., "The Ping-Pong Cannon: A Closer Look," *The Physics Teacher* **43**:22–25 (2005).

2. Cockman, J., "Improved Vacuum Bazooka," *The Physics Teacher* **41**:246–247 (2003).

3. Ayars, E., and Buchholtz, L., "Analysis of the Vacuum Cannon," *American Journal of Physics* **72**(7):961–963 (2004).

4. FLUENT, Web site: http://www.fluent.com [accessed 8 March 2007].

5. Anderson, J.D., *Modern Compressible Flow: With Historical Perspective*, McGraw-Hill Inc., (1989). ■